# Application of acyl-homoserine lactones for regulating biofilm characteristics on PAO1 and multi-strains in membrane bioreactor

Wonjung Song[1], Chehyeun Kim[2], Jiwon Han[2], Jihoon Lee[2], Zikang Jiang[2] and Jihyang Kweon[*2]

[1]*The Academy of Applied Science* and *Technology, Konkuk University, 120 Neungdong-ro, Gwangjin-gu, Seoul 05029, Republic of Korea*
[2]*Department of Environmental Engineering, Konkuk University, 120 Neungdong-ro, Gwangjin-gu, Seoul 05029, Republic of Korea*

**Abstract.** Biofilms significantly affect the performance of wastewater treatment processes in which biodegradability of numerous microorganisms are actively involved, and various technologies have been applied to secure microbial biofilms. Understanding changes in biofilm characteristics by regulating expression of signaling molecules is important to control and regulate biofilms in membrane bioreactor, i.e., biofouling. This study investigated effects of addition of acyl-homoserine lactones (AHL) as a controllable factor for the microbial signaling system on biofilm formation of *Pseudomonas aeruginosa* PAO1 and multiple strains in membrane bioreactor. The addition of three AHL, i.e., C4-, C6-, and C8-HSL, at a concentration of 200 μg/L, enhanced the formation of the PAO1 biofilm and the degree of increases in the biofilm formation of PAO1 were 70.2%, 76.6%, and 72.9%, respectively. The improvement of biofilm formation of individual strains by C4-HSL was an average of 68%, and the microbial consortia increased by approximately 52.1% in the presence of 200 μg/L C4-HSL. CLSM images showed that more bacterial cells were present on the membrane surface after the AHL application. In the COMSTAT results, biomass and thickness were increased up to 2.2 times (PAO1) and 1.6 times (multi-strains) by C4-HSL. This study clearly showed that biofilm formation was increased by the application of AHL to individual strain groups, including PAO1 and microbial consortia, and significant increases were observed when 50 or 100 μg/L AHL was administered. This suggests that AHL application can improve the biofilm formation of microorganisms, which could yield an enhancement in efficiency of biofilm control, such as in various biofilm reactors including membrane bioreactor and bioflocculent systems in water/wastewater treatment processes.

**Keywords:** acyl-homoserine lactones; biofilm formation; PVDF membrane; Quorum sensing

## 1. Introduction

Biofilms in wastewater treatment processes play an important role in improving contaminant removal because they protect microorganisms from hazardous environments. Therefore, favorable conditions for a robust and active biofilm are required in processes such as trickling filters and moving bed biofilm reactors (Chattopadhyay *et al.* 2022, Muhammad *et al.* 2020, Sehar and Naz 2016).

Biofilms formed by microorganisms have a complex matrix, and an understanding of structural changes and compositions due to the formation process or operational conditions is required to establish a designed biofilm for biological processes for specific objectives. Micro-organisms that reach a solid surface form biofilms through accumulation and growth. Microorganisms on the surface produce extracellular polymeric substances (EPS) and build a matrix around the perimeter of the organisms, forming a biofilm (Laspidou and Rittmann. 2002, Karyglanni *et al.* 2020, Costa *et al.* 2018 Shi *et al.* 2021). Biofilms are constructed using processes such as initial adhesion, consolidation, matrix formation, and detachment, and these processes are executed by a signal-response system, that is,

the quorum sensing (QS) system. QS is a cell-to-cell communication mechanism, and autoinducers are particular compounds that are essential for this signaling system. The signal compound for the QS system in gram-negative bacteria is acyl-homoserine lactone (AHL).

The role of autoinducers is associated with the cell density of microorganisms (Waters and Bassler 2005, Yeon *et al.* 2009). The "R" and "I" genes are homologs of the LuxR and LuxI genes. The "R" protein functions as an AHL receptor and a signal transducer. The "I" protein is a synthetase of the AHL signal. At certain bacterial cell levels, the quorum detection system is completely activated. This induces the R-mediated expression of quorum-detection target genes (Lade *et al.* 2014). In the presence of a high population of microorganisms, AHL secretion occurs, and when the concentration of AHL increases, it reverses diffusion into microbial cells and reacts with LuxI/LuxR, which initiates biofilm formation. In the biofilm formation process, high AHL concentrations in bulk at the initial stage of biofilm development can promote formation of biofilms by microorganisms and form a thick and mature biofilm, which indicates that regulating the AHL concentration can be an important control method to maintain efficiency in wastewater treatment processes.

The QS system also revealed a communication system that promotes generation of extracellular metabolites (Papenfort and Bassler 2016). Several processes in

∗Corresponding author, Professor,
E-mail: jhkweon@konkuk.ac.kr

wastewater treatment, such as activated sludge processes and aerobic granule sludge (AGS) systems, require active bio-flocculation, promoted by EPS. Technologies for enhancing the granulation of sludge have been increasingly applied, which apply various materials or substances to improve biomass retention and prevent sludge washout (Li *et al.* 2021). For instance, AGS processes enable the production of high suspended solid concentrations in reactors, compared to the conventional activated sludge process, and operate at shorter hydraulic residence times due to sludge with excellent bio-flocculent properties. The technology combining AGS and membrane bioreactor (MBR) offers significant advantages over conventional MBR processes for fouling reduction and wastewater treatment (Iorhemen *et al.* 2017). MBR has been applied in various fields such as water/wastewater treatment and water reuse of municipal and industrial wastewater due to its advantages of using biological treatment and membrane filtration. However, membrane fouling is a major process drawback that hinders MBR applications (Song *et al.* 2017). Recently, the application of granular biomass, such as AGS technology, has been attempted to mitigation of membrane fouling in MBR process (Wang *et al.* 2013, Bengtsson *et al.* 2019, Zhang *et al.* 2021). Efficient flocculation of the granular biomass is important for effective nutrient removal. Several studies have been conducted to evaluate the operating parameters for optimizing the granulation of sludge, however, the underlying mechanism of granulation and the effects of bioflocculent formation on granulation have not been fully understood (Wilén *et al.* 2018).

This study investigated the effects of AHL addition as a controllable factor for the microbial signaling system on biofilm formation and the possibility of biofilm control technology in wastewater treatment processes. The enhancement of biofilm formation was investigated by adding AHL, a major factor in biofilm formation in the QS system. Three short-chain AHLs (C4-HSL, C6-HSL, and C8-HSL) were applied. AHL with acyl chain lengths smaller than ten are called short-chain AHL, which play a role in the initial stage of biofilm development (Dobretsov *et al.* 2009, Mangwani *et al.* 2016, Muras *et al.* 2022). The application of AHL was performed in two different systems, that is, single *Pseudomonas aeruginosa* PAO1 and consortia of six strains, which were extracted from the sludge of a wastewater treatment plant and an MBR in practice. The MBR processes were selected because they have active bioflocs in the bulk and biofilm on the membrane surfaces. A mixed culture of six strains was used to extend the understanding of the effects of AHL addition on heterogeneous microbial cultures. Structural changes in the microbial biofilms were investigated using a Confocal Laser Scanning Microscopy (CLSM) analyzer. In biofilm research, surface observation using CLSM provides visualization of the biofilm structure, and structural factors of biofilms can be identified through quantification software using CLSM images. Programs such as COMSTAT (Heydornet *et al.* 2000) and Image Structure Analyzer (ISA) (Yang *et al.* 2000) have been developed to quantify each factor from a three-dimensional structure and are being applied to biofilm research.

## 2. Materials and methods

### 2.1 Bacterial strains and growth conditions

*Pseudomonas aeruginosa* PAO1 was selected as the single pure culture for biofilm formation. Six strains (*Pseudomonas aeruginosa* PAO1, *Pseudomonas aeruginosa* PA14, *Citrobacter freundii*, *Serratia marcescens*, *Aeromonas hydrophila*, and *Enterobacter ludwigii*) were used to create a consortium of heterogeneous microorganisms for biofilm formation. Previous studies have identified some strains that contribute to biofilm formation. Lade *et al.* (2014) reported that 12 isolates, including *Pseudomonas Aeromonas*, *Enterobacter*, *Serratia*, *Citrobacter*, and *Leclercia* were identified by nucleotide BLAST analysis of the 16SrRNA gene sequence from QS signal-producing bacterial isolates in a domestic wastewater treatment plant. PAO1 and PA14 were extracted from MBR-activated sludge, while *Citrobacter freundii*, *Serratia marcescens*, *Aeromonas hydrophila*, and *Enterobacter ludwigii* were obtained from KCCM and KCTC. Each strain was inoculated at 37°C in Luria-Bertani (LB) broth, nutrient broth, and trypticase soy broth (Difco BD, Franklin Lakes, NJ, USA) using each cultivation method.

### 2.2 Biofilm formation assay

A biofilm formation assay with a microtiter dish was used to evaluate the effects of AHL concentration on biofilm formation (O'Toole, 2011), with minor adjustments. Briefly, each strain was incubated for 18-24 hours under different culture conditions. Then, 100 µL aliquots of each suspension were added to 100 µL of fresh Luria-Bertani (LB) medium containing AHL in 96-well plates. After incubation at 37° C for 24 h, the plates were emptied and washed with D.I. Then, each well was stained with 200 µL of 0.1% crystal violet (CV) at room temperature for 20 min. To remove excess stains, the plates were washed three times again with D.I. The plate was soaked for 10 to 15 min in 200 µL of 30% acetic acid to lyse the remaining CVs. Then, the absorbance of solubilized CVs was measured at 550 nm for the biofilm formation capacity with a microplate reader (Synergy HT, Biotek, USA). Three AHLs (C4-HSL, C6-HSL, and C8-HSL) were purchased from Sigma-Aldrich (St. Louis, MO, USA).

### 2.3 Operation of CDC biofilm reactors

The effects of AHL addition on biofilm characteristics were investigated using a Center for Disease Control (CDC) biofilm reactor (BioSurface Technologies Corp., Bozeman, MT, USA). Prior to conducting the experiments for biofilm formation, the parts of CDC reactor (a reservoir for medium, polypropylene coupon holders, magnetic bars, and tubes) were autoclaved at 121 °C for 20 min. A commercial flat-sheet microfiltration membrane composed of polyvinylidene fluoride (PVDF) was purchased (Merck Millipore (Darmstadt, Germany). The membrane pore size was 0.22 µm, cut into 1.5 cm x 1.5 cm pieces, and sterilized using 40% ethanol, followed by UV light exposure for 1 h. The membrane specimen was fixed on one side of the

coupon holder. Eight rods were attached to the CDC reactor, and two membrane specimens were attached to each coupon rod. The CDC reactor was operated at 150 rpm for 24 hours. All the processes were conducted on a clean bench.

The CDC reactor was operated as follows: AHL concentrations of 20, 50, 100, and 200 μg/L were used. Since AHL exists with a very low concentration in the bulk, the AHL concentration range was selected for improve biofilm formation (Kim *et al.* 2013). The PAO1 culture or the multi-strains were incubated in 2.5 % LB broth and filled in the CDC reactors at a concentration of $10^6 \sim 10^7$ CFU/mL. The total volume of the mixture was 400 ml. A CDC reactor, as a blank control, was also operated under the same conditions without the addition of AHL. After 24 h of operation, the membranes were removed for EPS measurements and optical imaging analyses. The incubation time of 24 hrs was determined based on a pervious biofilm study with the CDC biofilm reactor (Percival *et al.* 2017).

### 2.4 Extracellular polymeric substance (EPS) extraction and *measurement*

EPS on the membrane surface was extracted using the cation exchange resin method (Frølund *et al.* 1996). The membrane specimens were carefully removed from CDC rods. The residue on the membrane surface was washed with 20 mL of phosphate-buffered saline. After washing, the membrane was transferred to a conical tube containing 40 mL buffer solution, vortexed for 5 min, and sonicated for 60 min (B5510, Branson Ultrasonics, USA). After detaching the biofilm from the membrane, it was removed from the conical tube. CER was added at a ratio of 5 g CER per 60-80 cm$^2$ of membrane surface (Al-Halbouni *et al.* 2008). A solution including CER was stirred at 600 - 900 rpm for 1.5 hours at a temperature of 4 °C. Then, the CER in the solution was separated using a 0.45-μm filter. Extracted EPS were analyzed for polysaccharides and proteins.

Proteins were quantified using Bradford assay. Briefly, a standard curve was obtained using different concentrations of bovine serum albumin (BSA). Standard solutions were prepared by diluting a stock solution with 2 mg/mL BSA in the range of 0–10 μg/mL, and the absorbance was analyzed for protein quantification. A Protein Assay Kit (BR500, Bio-Rad, USA) was used to analyze the BSA solutions and extracted EPS samples. Each sample and 1 mL of protein dye was placed in a microcuvette and allowed to stand for 10 min. Absorbance was measured at 595 nm. The protein content of the samples was calculated from the absorbance data of the standard solutions. A UV/vis spectrophotometer (DR 6000, HACH, USA) was used for the absorbance measurements. Polysaccharide quantification was performed using a TOC analyzer (SIEVERS 5310C, GE, Australia).

### 2.5 Confocal laser scanning microscopy (CLSM) observation

Confocal laser scanning microscopy (CLSM) analysis was performed to observe biofilms on the membrane surfaces. The three-dimensional information of the biofilm including live cells and dead cells can be configured through CLSM analysis images, and factors such as biomass, surface-to-biovolume ratio, thickness, and roughness can be quantified through the image analysis program. The experimental methods were described by Lade *et al.* (2017). Briefly, the detached membranes were dyed for 30 min with 200 μL of the LIVE/DEAD BacLight bacterial viability kit (Molecular Probes, Eugene, OR, USA) and wrapped in aluminum foil to block light. The excess stain was carefully washed with deionized sterile water, and the membranes were mounted on glass slides (covered with a coverslip). Microscopic observation and image acquisition were performed on stained membranes using a confocal laser scanning microscope (LSM 800, ZEISS, Germany). The membrane surface was observed at 20 × magnification using a CLSM. The observed area was $1024 \times 1024\,\mu m^2$ with a resolution of $1024 \times 1024$ pixels. The biofilm structure was quantified from the confocal stack using the COMSTAT image analysis software. In this study, the biofilm differences generated under each condition were determined using the four COMSTAT parameters. These parameters were total biomass, surface-to-biovolume ratio (SBR), mean thickness, and roughness coefficient.

The total biomass ($\mu m^3/\mu m^2$) was obtained from the number of biomass pixels in all images multiplied by the unit volume of the pixel and divided by the substratum area. The SBR ($\mu m^2/\mu m^3$) is the ratio of all surfaces exposed to voids, which reflects the fraction of the biofilm exposed to nutrient flow. The mean thickness (μm)is a calculation of the thickness distribution of the biofilm per pixel column, while the uncovered areas were not calculated. The roughness coefficient (-) indicates the variability in the measured biofilm thickness (Murga *et al.* 1995). The formula for the calculation is as follows:

$$R_a^* = \frac{1}{N} \sum_{i=1}^{N} \frac{\left| L_{fi} - \overline{L_f} \right|}{\overline{L_f}} \tag{1}$$

where $Lfi$ is the i-th measured individual thickness, $Lf$ is the average thickness, and N is the number of thickness measurements.

### 2.6 Statistical analysis

Statistical analysis of biofilm formation was performed using Microsoft Excel software (Microsoft, Redmond, WA, USA). The values presented are means of three repeated experiments with standard deviations indicated in error bars.

## 3. Results and Discussion

### 3.1 Improving formation of Pseudomonas Aeruginosa biofilm

#### 3.1.1 Effects of AHL doses on biofilm formation

A biofilm formation assay was performed to examine PAO1 biofilm development caused by the addition of AHL.

(a) C4-HSL
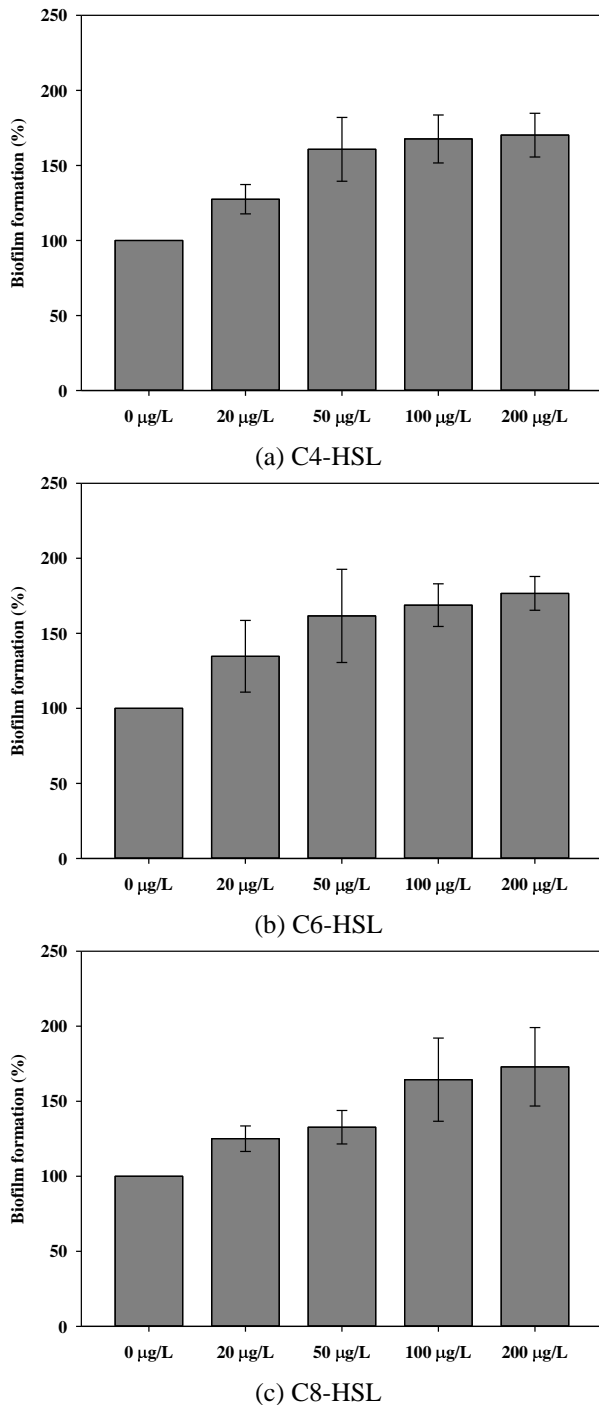


(b) C6-HSL



(c) C8-HSL

Fig. 1 Effects of AHL chain-length and different concentration on PAO1 biofilm formation (n=3)

Doses of 0, 20, 50, 100, and 200 µg/L were used for C4-HSL, C6-HSL, and C8-HSL, respectively. An increasing pattern of biofilm formation was observed in all cases. The C4-HSL addition showed biofilm formation of 127.5, 160.8, 167.7, and 170.2% with increasing doses, compared to the dose of 0 µg/L. C6-HSL showed a similar pattern to that of C4-HSL. Biofilm formation by C6-HSL addition was increased by 34.7, 61.6, 68.8, 76.6% as 20, 50, 100, and 200 µg/L of C6-HSL. With the application of C8-HSL, the increase of the biofilm was 25.1% at 20 µg/L,

32.7% at 50 µg/L, 64.4% at 100 µg/L, and 73.0% at 200 µg/L. At a dose of 200 µg/L, the AHL addition improved biofilm formation by more than 70%. The trend in biofilm formation by C4-HSL was similar to that of C6-HSL. Biofilm formation increased significantly at lower doses and reached a constant rate at doses higher than 50 µg/L. The biofilm of PAO1 with C8-HSL addition showed an increase in biofilm to a dose of 100 µg/L, and the rate of increase seemed to decrease at a dose of 120 µg/L.

Zhu *et al.* (2019) reported an improvement in biofilm formation by the application of 150 µg/ml C4-HSL in *Hafnia alvei* H4, which is a common food contaminant that has been frequently isolated from spoiled food products. Morohoshi *et al.* (2007) observed that the biofilm formation was increased by approximately 62% over parental biofilm levels by 5 µM of exogenous C6-HSL addition to *Serratia marcescens* AS-1. Our study revealed that the enhancement of PAO1 biofilm formation occurred at a relatively low dose of short-chain AHL, that is, C4-HSL, C6-HSL, and C8-HSL.

### 3.1.2 Comparision of biofilm characteristics by AHLs with different chain lengths on PVDF membrane surfaces

The CDC reactor was operated to characterize the effects of different AHL chain lengths. The three AHL were administered at 50 µg/L. After CDC reactor operation was completed, the biofilm on the PVDF membrane surfaces was examined using CLSM. Visualization of clustering patterns or particular shapes of biofilm structures in the biofilm was performed using CLSM images. Lynch *et al.* (2002) reported using CLSM images that the ability to generate microcolony structures was partially restored when 10 µM C4-HSL was administered to the *Aeromonas hydrophila* ahyI mutant.

Fig. 2 shows the PAO1 biofilm on the membrane surface with the three AHLs. The CLSM image of the control, in which AHL was not applied, was also evaluated. The image shows live cells in green and dead cells in red. The image of the control reactor shows some empty space, and the membrane surface is covered with less biomass. On the other hand, under the conditions of AHL application, it was observed that the membrane surface was more and thickly covered with biomass composed of live and dead cells than that of the control reactor.

CLSM images were quantified by factors such as total biomass, surface to biovolume ratio (SBR), mean thickness, and roughness coefficient using an image quantitation analysis, that is, COMSTAT (An and Parsek 2007, Reichhardt and Parsek 2019). The total biomass showed an increase in the number of microorganisms on the membrane surface after AHL application. In addition, the total biomass increased as the chain length of AHL increased. The total biomass under each condition was $11.00 \pm 6.49$, $15.92 \pm 7.36$, $18.63 \pm 10.47$, and $24.06 \pm 7.87$ µm$^3$/µm$^2$. The mean thickness showed a large increase upon the application of C8-HSL. The mean thickness increased by 0.05 µm and 4.56 µm under the conditions of C4- and C6-HSL, respectively. However, the mean thickness increased approximately 1.8 times to 41.82 µm with C8-HSL application.
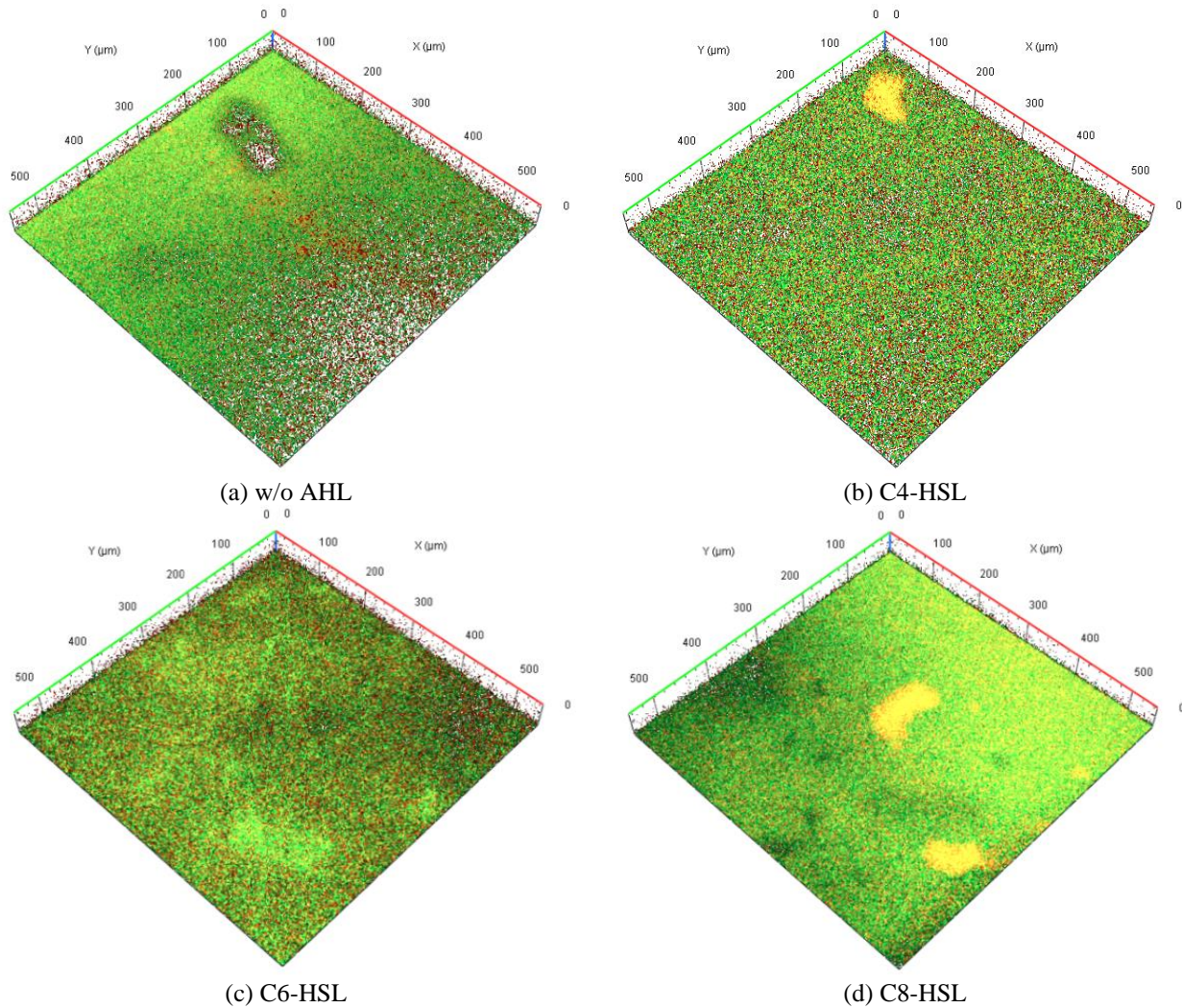
(a) w/o AHL

(b) C4-HSL

(c) C6-HSL

(d) C8-HSL

Fig. 2 Variations of three-dimensional structures of biofilm: effects of the chain-length in AHL (green: live cell, red: dead cell)

Table 1 Biofilm properties from COMSTAT analysis: effects of the chain-length in AHL

|  | Total biomass ($\mu m^3\ \mu m^{-2}$) | Surface to biovolume ratio ($\mu m^2\ \mu m^{-3}$) | Mean thickness ($\mu m$) | Roughness coefficient (-) |
|---|---|---|---|---|
| w/o AHL | $11.00 \pm 6.49$ | $5.48 \pm 0.20$ | $23.46 \pm 0.53$ | $1.06 \pm 0.21$ |
| w/ C4- HSL | $15.92 \pm 7.36$ | $5.46 \pm 1.02$ | $23.51 \pm 11.19$ | $0.99 \pm 0.48$ |
| w/ C6- HSL | $18.63 \pm 10.47$ | $5.04 \pm 1.44$ | $28.02 \pm 14.26$ | $0.87 \pm 0.58$ |
| w/ C8- HSL | $24.06 \pm 7.87$ | $4.05 \pm 1.00$ | $41.82 \pm 10.07$ | $0.23 \pm 0.43$ |

### 3.2 Effects of C4-HSL on biofilm formation by various microorganisms

Various microorganisms are involved in the formation of water biofilms, such as biofilms on membrane surfaces, supply pipe materials, and aerobic or anaerobic granules. The biofilm-formation properties of C4-HSL were investigated using various strains of water biofilms. Six strains were identified from the MBR and the activated sludge, including *Pseudomonas aeruginosa* PAO1, *Pseudomonas aeruginosa* PA14, *Citrobacter freundii*, *Serratia marcescens*, *Aeromonas hydrophila*, and *Enterobacter ludwigii*. Six strains were used in the biofilm

formation assay, as shown in Fig. 3. Biofilm formation was increased by C4-HSL application, which was obvious with the rising pattern of the bar graph.

The biofilm formation showed an increase by up to 40.9% at 20 µg/L addition, up to 65.5% at 50 µg/L application, up to 90.4% at the 100 µg/L condition and up to 94.4% at the 200 µg/L application. The results for PAO1 biofilm are described in the previous section, which were improved by 27.5% by C4-HSL of 20 µg/L, and by 60.8 and 67.7% at 50 and 100 µg/L, respectively. Among the strains tested, PA14 showed the greatest enhancement in biofilm formation. The biofilm formation of PA14 was increased by 40.9, 59.9, 90.4, and 94.4% with 20, 50, 100,

(a) PAO1                (b) PA14

(c) *C. freundii*          (d) *S. marcescens*

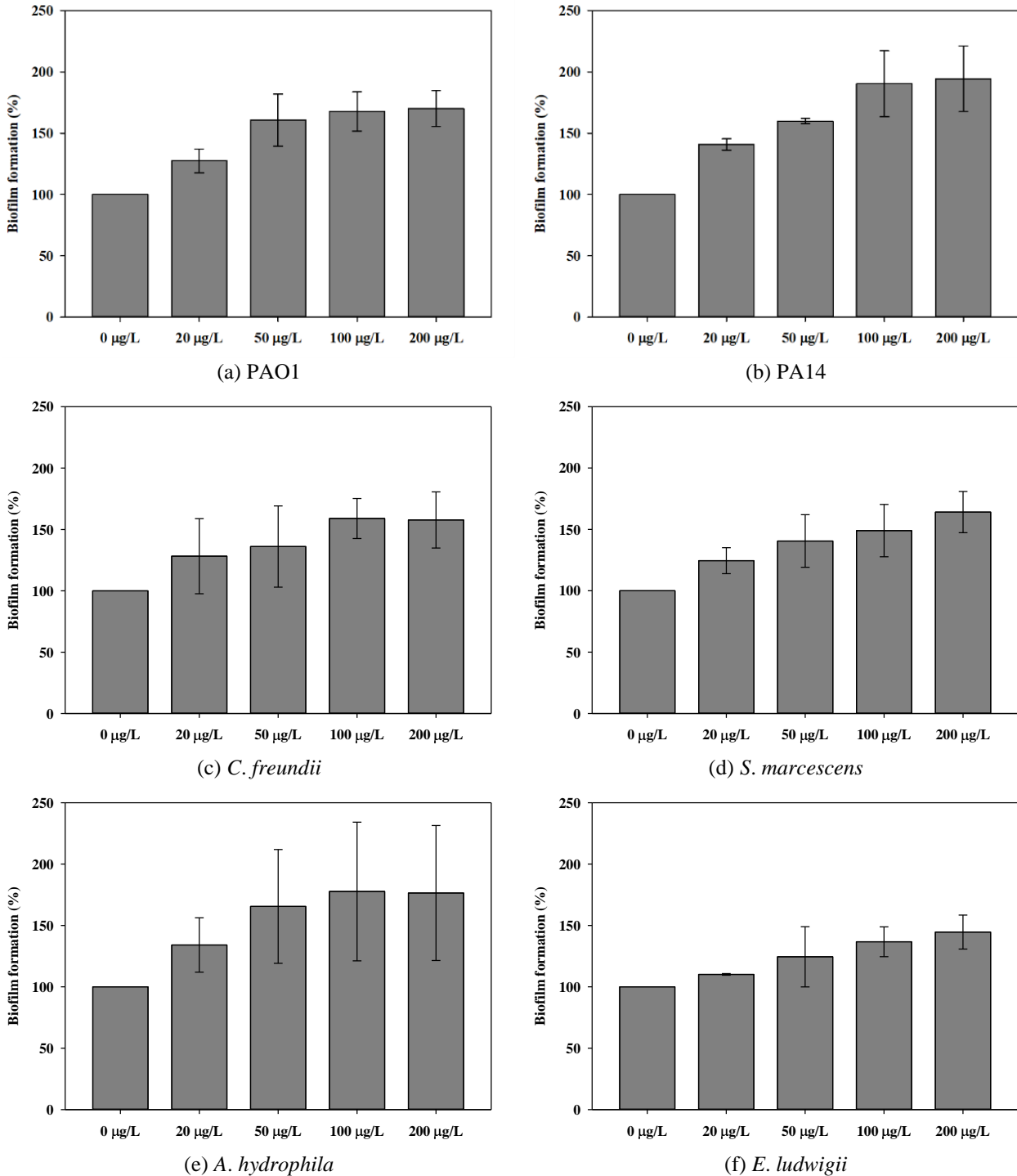(e) *A. hydrophila*         (f) *E. ludwigii*

Fig. 3 Effect of different C4-HSL concentration on biofilm formation (n=3)

and 200 µg/L C4-HSL doses, respectively. *C. freundii* increased by 28.2 and 36.1% at 20 and 50 µg/L C4-HSL, respectively. When the dosing concentrations exceeded 100 µg/L, it increased by more than 50%, 100 µg/L by 59.0%, and 200 µg/L by 57.7%. *S. marcescens* showed an increase by 24.5, 40.6, 49.0, and 64.1% with C4-HSL, whereas *A. hydrophila* showed an increase of 34.1, 65.6, 77.7, and 76.5%, and biofilm formation improved by 65.6% when dosing concentration was 50 µg/L or higher. *E. ludwigii* showed the lowest biofilm formation improvement among the strains. It showed 10.1, 24.5, 36.7, and 44.6% under the conditions of 20, 50, 100, and 200 µg/L C4-HSL.

High rates of increase occurred at doses lower than 50 µg/L or 100 µg/L depending on the strain, such as PAO1, PA14, *C. freundii*, and *A. hydrophila*. The strains of *S. marcescens* and *E. ludwigii* showed a linear increase in biofilm formation as the C4-HSL concentration increased.

A correlation was observed between the applied concentration range of C4-HSL and biofilm formation, as shown in Fig. 4. The correlation was obtained for the entire

(a) Concentration range 0 to 200 µg/L



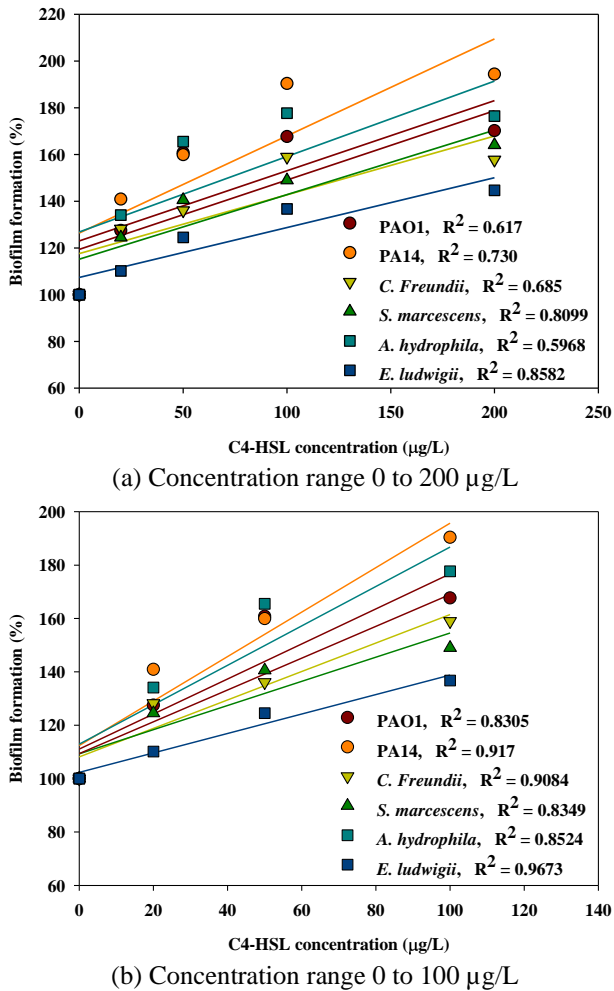(b) Concentration range 0 to 100 µg/L

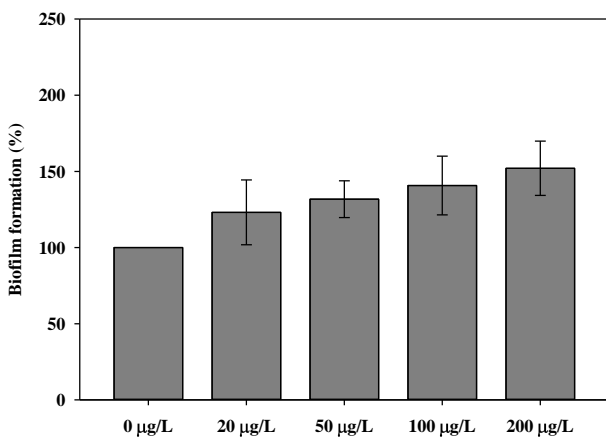Fig. 4 Correlation between C4-HSL concentration and biofilm formation



Fig. 5 Effect of C4-HSL on biofilm formation by microbial consortia (n=3)

range of doses in Fig. 4(a) and with doses up to 100 µg/L, as shown in Fig. 4(b). The correlation coefficient up to 100 µg/L was much higher than that for the entire range of applied concentrations. In the concentration range of 0–200 µg/L, the average correlation coefficient of the six strains was 0.727. The correlation coefficient between C4-HSL

concentration and biofilm formation by single strains was lowest in *A. hydrophila* (0.597) and highest in *E. ludwigii* (0.858). However, considering the concentration range up to 100 µg/L, the average correlation of the six strains increased to 0.885. The strain with the highest correlation was *E. ludwigii*, with a correlation coefficient of 0.967, and PA14 showed the lowest correlation coefficient of 0.831. The regulation of water biofilms with the designed properties was likely affected by the applied doses of AHL. A proper dose should be sought for efficient biofilm control.

### 3.3 C4-HSL addition to consortia of microorganisms

#### 3.3.1 Effects of C4-HSL on biofilm formation

The effects of C4-HSL addition on biofilm formation by consortia of microbial cells were observed. The variations in biofilm formation are shown in Fig. 5. The applied C4-HSL concentrations were 20, 50, 100, and 200 µg/L, respectively. The C4-HSL addition affected biofilm formation by microbial consortia, as shown by the higher level of biofilm formed by AHL application compared with non-AHL dosing.

Microbial consortia biofilm formation increased linearly with increasing concentrations of C4-HSL. The biofilm formation increases under C4-HSL-applied conditions were 23.1%, 31.8%, 40.7%, and 52.1%, respectively. The increase in biofilm formation by microbial consortia was dampened compared to that by the single strain of PAO1. At a concentration of 200 µg/L, the increase was 70.2% for the PAO1 biofilm. Biofilm formation by the six individual strains showed that five strains, except *E. ludwigii* also showed greater biofilm formation than the microbial consortia. It probably due to the fact that an increase in complex behavioural patterns or a competition for dominance between strains was occurred in the mixed culture or during the culturing process (Burmølle *et al.* 2006). In biofilms with multiple heterogeneous species, different species biofilms can be colonized or inhibited by competition (Stewart *et al.* 2012).

#### 3.3.2 Variation in extracellular polymeric substances of biofilm

The EPS variation was evaluated using five different doses of C4-HSL. EPS excretion during biofilm development is critical, and the composition of EPS determines the properties of the biofilm. The EPS played a key role as a medium, allowing the aggregation of microorganisms and stable proximity of the bacteria, thus constructing biofilms (Ryu *et al.* 2021). The major components of the EPS are proteins and polysaccharides. Proteins are known to be more involved in stabilizing aggregate structures than polysaccharides. The variation in EPS composition with the addition of C4-HSL at different concentrations is shown in Fig. 6.

With C4-HSL application, the EPS on the membrane surface showed a change in its composition. The amount of protein in the biofilm increased after C4-HSL administration. A relatively linear increase was observed as the dosing concentration increased, except for the great surge at a dose of 20 µg/L. Under each condition, the

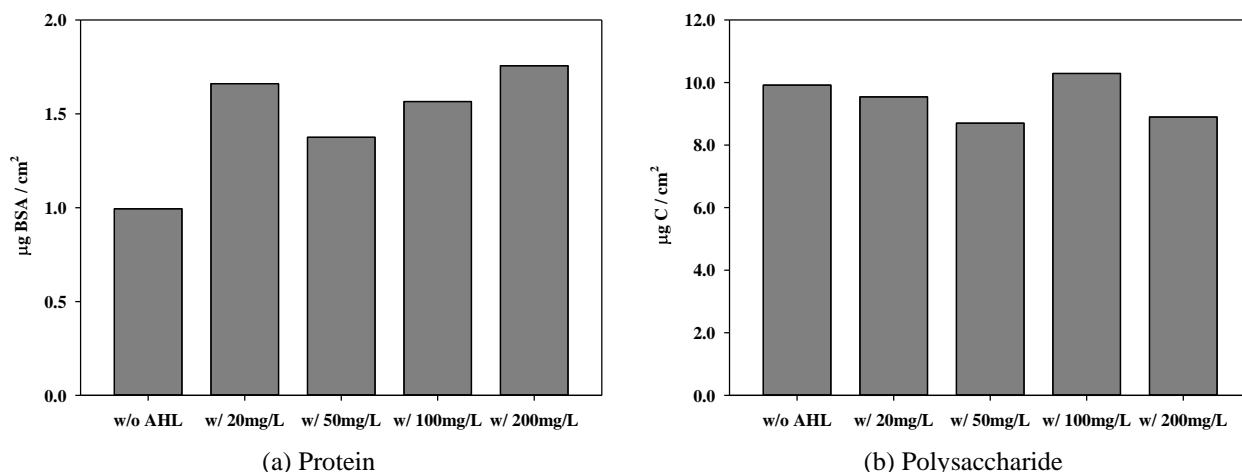|                      (a) Protein                      |                      (b) Polysaccharide                      |

Fig. 6 Effect of C4-HSL on EPS composition by microbial consortia (n=1)

Table 2 Quantification of microbial consortia biofilm structure by COMSTAT program: effect of C4-HSL concentration

|  | Total biomass ($\mu m^3$ $\mu m^{-2}$) | Surface to biovolume ratio ($\mu m^2$ $\mu m^{-3}$) | Mean thickness ($\mu m$) | Roughness coefficient (-) |
|---|---|---|---|---|
| w/o C4-HSL | 13.85 ± 1.97 | 5.32 ± 0.08 | 23.43 ± 0.06 | 1.00 ± 0.00 |
| w/ 20 µg/L | 22.01 ± 2.06 | 4.88 ± 1.01 | 28.58 ± 10.23 | 0.99 ± 0.02 |
| w/ 50 µg/L | 18.37 ± 4.49 | 5.34 ± 0.02 | 23.38 ± 0.11 | 1.00 ± 0.00 |
| w/ 100 µg/L | 19.28 ± 6.54 | 5.34 ± 0.06 | 23.48 ± 0.03 | 1.00 ± 0.00 |

protein levels increased to 0.99, 1.66, 1.38, 1.57, and 1.76 µg BSA/cm². The polysaccharides were maintained at a similar amount with no particular pattern. Without C4-HSL dosing, the polysaccharide content was 9.92 µg C/cm². The amount was changed to 9.54, 8.70, 10.29, and 8.90 µg BSA/cm² at doses of 20, 50, 100, and 200 µg/L, respectively.

Tan *et al*. (2014) reported that the exogenous AHLs addition, such as 3OC6-HSL, 3OC8-HSL, and 3OC12-HSL, as well as the unsubstituted C6-HSL, to the sludge of aerobic granules can enhance the EPS production, and the polysaccharide and protein increase by up to 36% and 16%, respectively. The authors also indicated that C8-HSL and C12-HSL had no effect on the total EPS production after 1 h of incubation. This study revealed that the protein showed a significant increase, which was approximately 80%, but the polysaccharide content only increased by 4% with 100 µg/L of C4-HSL. The effects of AHLs addition on the assembly of the sludge community were seemingly specific to the types of AHLs and their surrounding environments.

### 3.3.3 Biofilm structural characteristics

CLSM images of the biofilm by the microbial consortia were analysed along with EPS measurements. In addition, the structural characteristics of the biofilms were evaluated and are summarized in Table 2. Figure 7 shows the biofilm change on the membrane surface caused by C4-HSL addition. The number of microbial cells on the membrane surface increased as the concentration of applied C4-HSL increased. Microbial cells appeared to significantly increase under conditions of 20 and 200 µg/L C4-HSL application.

The CLSM image without C4-HSL (Fig (a)) shows several voids on the membrane surface that were not covered with biomass. The voids were observed in white, while other areas were visualized with green colour for live cells or red colour for dead cells. The application of C4-HSL led to an increase in biomass in the observation area. With the application of 20 µg/L of C4-HSL application (Fig (b)), the intensity of the CLSM image was high, which was attributed to the increased biomass on the surface. A small decrease in biomass was observed at 50 µg/L C4-HSL (Fig (c)), but as the concentration increased to 100 and 200 µg/L, decreases in voids on the membrane surface and increases in biomass were observed.

Table 2 presents the COMSTAT data, which can be used to understand the variation in biofilm structural factors by different C4-HSL concentrations for biofilms produced by the microbial consortia. Compared to the control experiment with a dose of 0 µg/L C4-HSL, all quantification data of the experiments with C4-HSL dosing showed increases in the total biomass, surface-to-biovolume ratio, mean thickness, and roughness coefficient. However, this variation was not dose-dependent. The highest total biomass was observed at the dose of 20 µg/L. The mean thickness also showed the highest value at a dose of 20 µg/L, and the thickness at the other doses was similar to that of the control experiment. The total biomass increased to 22.01 µm³/µm², and the mean thickness was 28.58 µm, approximately 59.0% and 22.0% increases, respectively. Under the conditions of 50 and 100 µg/L of C4-HSL, all factors of COMSTAT were similar or higher than those of the control. The total biomass was 18.37 ± 4.47 µm³/µm² when 50 µg/L of

(a) 0 µg/L

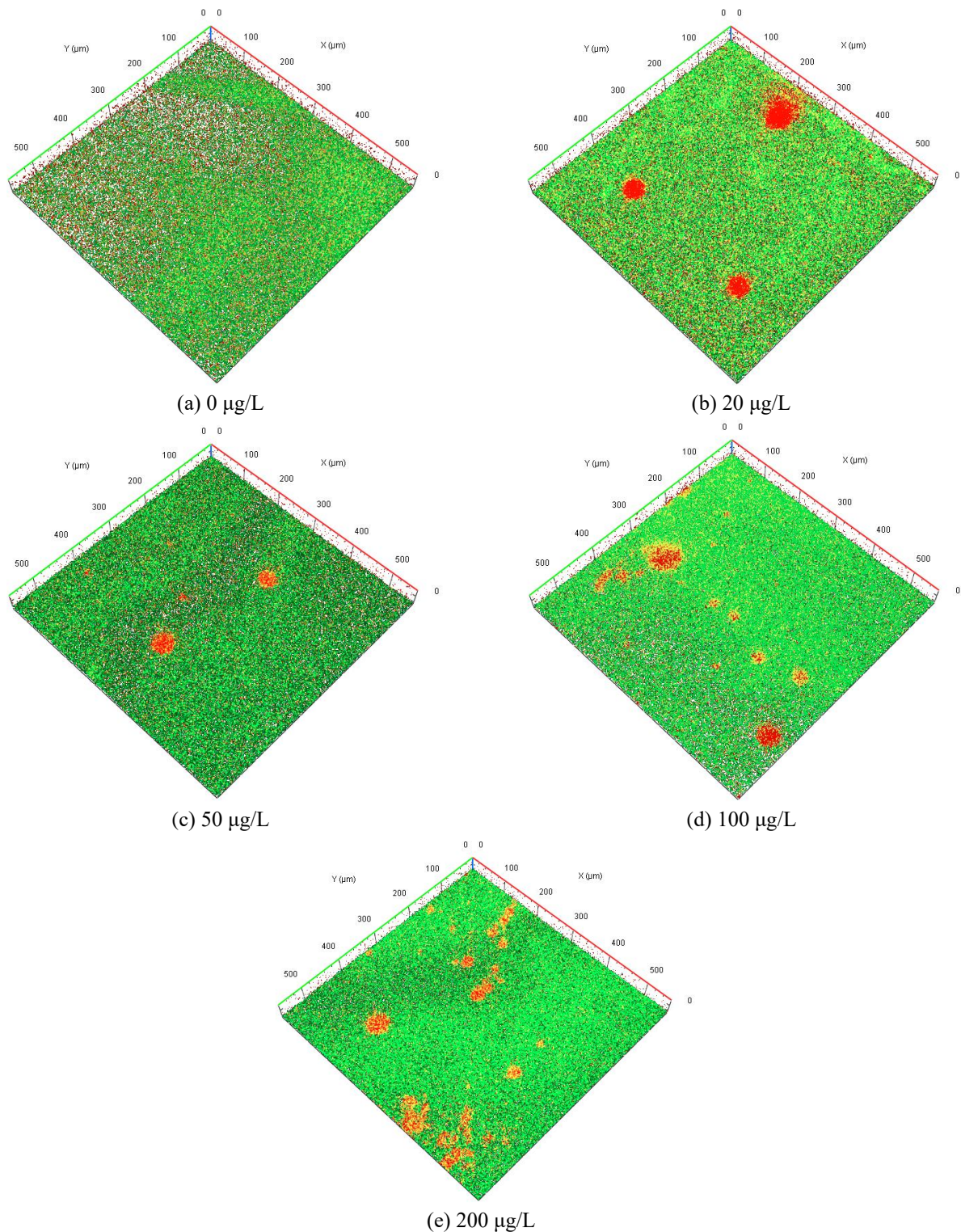(b) 20 µg/L

(c) 50 µg/L

(d) 100 µg/L

(e) 200 µg/L

Fig. 7 Effect of different C4-HSL concentration on microbial consortia biofilm structure

C4-HSL was added. 200 µg/L of C4-HSL increased total biomass to $19.28 \pm 6.54$ µm³/µm². Under conditions of 50 and 100 µg/L C4-HSL, the mean thickness did not show a significant increase or decrease. When 50 µg/L C4-HSL was applied, the mean thickness was $23.38 \pm 0.11$ µm, showing the lowest value. The mean thickness of 100 µg/L C4-HSL was $23.48 \pm 0.03$ µm.

The variation in the biofilm structural factors by the microbial consortia was somewhat reduced compared to that of the PAO1 biofilm, as presented in Table 1. The total biomass of the PAO1 biofilm changed from $11.00 \pm 6.50$ µm³/µm² with the addition of AHL to a maximum of $24.06 \pm 7.87$ µm³/µm² with 50 µg/L C8-HSL. This increase was approximately 118.8%, which was much greater than the

data shown in Table 1. The assembly of the various strains in the microbial consortia played individual roles in the biofilm, thus, the interplay of the consortia resulted in a stable biofilm, although the high values of total biomass and the mean thickness were inevitable due to the increases in the signal compound concentrations.

## 4. Conclusions

In this study, the effects of AHL addition on biofilm formation as a controlling factor of the microbial signaling system were investigated to evaluate the effect of AHL dosing on biofilm control technology in various wastewater treatment processes. The enhancement of biofilm formation was examined using biofilm formation potential, CLSM observations, and EPS analysis. AHL was applied in two different systems (PAO1 and a consortium of six strains) at concentrations of 0, 20, 50, 100, and 200 μg/L. AHL application enhanced biofilm formation on the PVDF membrane surface and induced changes in biofilm structure and EPS composition. The conclusions drawn from this study are as follows.

• The addition of AHLs to the culture of microbes appeared to cause an increase in biofilm formation. The three types of AHL used in this study improved biofilm formation by more than 70% at a concentration of 200 μg/L. Biofilm formation was increased by C4-HSL in six strains and showed a large increase when dosed at 50 or 100 μg/L.

• The 3D images from CLSM analyses and the quantitative analyses using COMSTAT show variation in the biofilm formed on the PVDF membrane surface with AHL application. AHL, with a longer chain length, induced an increase in the total biomass and mean thickness of the PAO1 biofilm. In addition, 200 μg/L C4-HSL induced the formation of compact multi-strain biofilms.

• The changes in EPS composition caused by AHL had a greater effect on proteins than on polysaccharides. The protein content increased by up to 56.2%% with 200 μg/L C4-HSL, and the polysaccharide content increased by only 3.6% with 100 μg/L C4-HSL.

This study implied that improvement in exploring QS strategies could yield great efficiency of biofilm control such as various biofilm reactors. In addition, the enhanced biofilm formation by the AHL application is expected to help the aggregation of bacteria in the bioflocculent systems of activated sludge or MBR sludge in water/wastewater treatment processes. Effective methods for biofilm control with AHL and applicability to the processes should be further investigated to enhance biological treatment performance.

## Acknowledgments

## References

Al-Halbouni, D., Traber, J., Lyko, S., Wintgens, T., Melin, T., Tacke, D., Janot, A., Dott, W. and Hollender, J. (2008), "Correlation of EPS content in activated sludge at different sludge retention times with membrane fouling phenomena", *Water Res.*, **42**(6-7), 1475-1488. https://doi.org/10.1016/j.watres.2007.10.026

An, D. and Parsek, M.R. (2007), "The promise and peril of transcriptional profiling in biofilm communities", *Curr. Opinion Microbiol.*, **10**(3), 292-296. https://doi.org/10.1016/j.mib.2007.05.011

Bengtsson, S., de Blois, M., Wilén, B.M. and Gustavsson, D. (2019). A comparison of aerobic granular sludge with conventional and compact biological treatment technologies. *Environ. Technol.*, **40**(21), 2769-2778. https://doi.org/10.1080/09593330.2018.1452985

Burmølle, M., Webb, J.S., Rao, D., Hansen, L.H., Sørensen, S.J. and Kjelleberg, S. (2006), "Enhanced biofilm formation and increased resistance to antimicrobial agents and bacterial invasion are caused by synergistic interactions in multispecies biofilms", *Appl. Environ. Microbiol.*, **72**(6), 3916-3923. https://doi.org/10.1128/AEM.03022-05

Chattopadhyay, I., Usman, T.M. and Varjani, S. (2022), "Exploring the role of microbial biofilm for industrial effluents treatment", *Bioengineered*, **13**(3), 6420-6440. https://doi.org/10.1080/21655979.2022.2044250

Costa, O.Y., Raaijmakers, J.M. and Kuramae, E.E. (2018), "Microbial extracellular polymeric substances: ecological function and impact on soil aggregation", *Front. Microbiol.*, **9**, 1636. https://doi.org/10.3389/fmicb.2018.01636

Dobretsov, S., Teplitski, M. and Paul, V. (2009), "Mini-review: quorum sensing in the marine environment and its relationship to biofouling", *Biofouling*, **25**(5), 413-427. https://doi.org/10.1080/08927010902853516

Frølund, B., Palmgren, R., Keiding, K. and Nielsen, P.H. (1996), "Extraction of extracellular polymers from activated sludge using a cation exchange resin", *Water Res.*, **30**(8), 1749-1758. https://doi.org/10.1016/0043-1354(95)00323-1

Heydorn, A., Nielsen, A.T., Hentzer, M., Sternberg, C., Givskov, M., Ersbøll, B.K. and Molin, S. (2000), "Quantification of biofilm structures by the novel computer program COMSTAT", *Microbiology*, **146**(10), 2395-2407. https://doi.org/10.1099/00221287-146-10-2395

Iorhemen, O.T., Hamza, R.A. and Tay, J.H. (2017). Membrane fouling control in membrane bioreactors (MBRs) using granular materials. *Bioresour. Technol.*, **240**, 9-24. https://doi.org/10.1016/j.biortech.2017.03.005

Karygianni, L., Ren, Z., Koo, H. and Thurnheer, T. (2020), "Biofilm matrixome: extracellular components in structured microbial communities", *Trends Microbiol.*, **28**(8), 668-681. https://doi.org/10.1016/j.tim.2020.03.016

Kim, S.R., Oh, H.S., Jo, S.J., Yeon, K.M., Lee, C.H., Lim, D.J., Lee, C.H. and Lee, J.K. (2013), "Biofouling control with bead-entrapped quorum quenching bacteria in membrane bioreactors: Physical and biological effects", *Environ. Sci. Technol.*, **47**(2), 836-842. https://doi.org/10.1021/es303995s

Lade, H., Paul, D. and Kweon, J.H. (2014), "Isolation and molecular characterization of biofouling bacteria and profiling of quorum sensing signal molecules from membrane bioreactor activated sludge", *Int. J. Mol. Sci.*, **15**(2), 2255-2273. https://doi.org/10.3390/ijms15022255

Lade, H., Paul, D. and Kweon, J.H. (2014), "Quorum quenching mediated approaches for control of membrane biofouling", *Int. J. Biol. Sci.*, **10**(5), 550. https://doi.org/10.7150/ijbs.9028.

Lade, H., Song, W.J., Yu, Y.J., Ryu, J.H., Arthanareeswaran, G. and Kweon, J.H. (2017), "Exploring the potential of curcumin

for control of N-acyl homoserine lactone-mediated biofouling in membrane bioreactors for wastewater treatment", *RSC Adv.*, **7**(27), 16392-16400. https://doi.org/10.1039/C6RA28032C

Laspidou, C.S. and Rittmann, B.E. (2002), "A unified theory for extracellular polymeric substances, soluble microbial products, and active and inert biomass", *Water Res.*, **36**(11), 2711-2720. https://doi.org/10.1016/S0043-1354(01)00413-4

Li, Y.Y., Huang, X.W. and Li, X.Y. (2021), "Use of a packed-bed biofilm reactor to achieve rapid formation of anammox biofilms for high-rate nitrogen removal", *J. Clean. Prod.*, **321**, 128999. https://doi.org/10.1016/j.jclepro.2021.128999

Lynch, M.J., Swift, S., Kirke, D.F., Keevil, C.W., Dodd, C.E. and Williams, P. (2002), "The regulation of biofilm development by quorum sensing in Aeromonas hydrophila", *Environ. Microbiol.*, **4**(1), 18-28.
https://doi.org/10.1046/j.1462-2920.2002.00264.x

Mangwani, N., Kumari, S. and Das, S. (2016), "Effect of synthetic N-acylhomoserine lactones on cell–cell interactions in marine Pseudomonas and biofilm mediated degradation of polycyclic aromatic hydrocarbons", *Chem. Eng. J.*, **302**, 172-186. https://doi.org/10.1016/j.cej.2016.05.042

Morohoshi, T., Shiono, T., Takidouchi, K., Kato, M., Kato, N., Kato, J. and Ikeda, T. (2007), "Inhibition of quorum sensing in Serratia marcescens AS-1 by synthetic analogs of N-acylhomoserine lactone", *Appl. Environ. Microbiol.*, **73**(20), 6339-6344. https://doi.org/10.1128/AEM.00593-07

Muhammad, M. H., Idris, A.L., Fan, X., Guo, Y., Yu, Y., Jin, X., Qiu, J., Guan, X. and Huang, T. (2020), "Beyond risk: bacterial biofilms and their regulating approaches", *Front. Microbiol.*, **11**, 928. https://doi.org/10.3389/fmicb.2020.00928

Muras, A., Mayer, C., Otero-Casal, P., Exterkate, R.A., Brandt, B.W., Crielaard, W., Otero, A. and Krom, B.P. (2020), "Short-Chain N-acylhomoserine lactone quorum-sensing molecules promote periodontal pathogens in in vitro oral biofilms", *Appl. Environ. Microbiol.*, **86**(3), e01941-19. https://doi.org/10.1128/AEM.01941-19

Murga, R., Stewart, P.S. and Daly, D. (1995), "Quantitative analysis of biofilm thickness variability", *Biotechnol. Bioeng.*, **45**(6), 503-510. https://doi.org/10.1002/bit.260450607

O'Toole, G.A. (2011), "Microtiter dish biofilm formation assay", *JoVE J. Visual. Experim.*, **47**, e2437.
https://doi.org/10.3791/2437

Papenfort, K and Bassler, B.L. (2016), "Quorum sensing signal–response systems in Gram-negative bacteria", *Nature Rev. Microbiol.*, **14**(9), 576.
https://doi.org/10.1038%2Fnrmicro.2016.89

Reichhardt, C. and Parsek, M.R. (2019), "Confocal laser scanning microscopy for analysis of Pseudomonas aeruginosa biofilm architecture and matrix localization", *Front. Microbiol.*, **10**, 677. https://doi.org/10.3389/fmicb.2019.00677

Percival, S.L., Mayer, D. and Salisbury, A.M. (2017), "Efficacy of a surfactant-based wound dressing on biofilm control", *Wound Repair Regenerat.*, **25**(5), 767-773.
https://doi.org/10.1111/wrr.12581

Ryu, J., Jung, J., Park, K., Song, W., Choi, B. and Kweon, J., (2021) "Humic acid removal and microbial community function in membrane bioreactor", *J. Hazard. Mater.*, **417**, 126088. https://doi.org/10.1016/j.jhazmat.2021.126088.

Sehar, S. and Naz, I. (2016), "Role of the biofilms in wastewater treatment", *Microbial Biofilms-importance Applicat.*, 121-144. http://doi.org/10.5772/63499

Shi, S., Zhang, Y., Tang, Q. and Mo, J. (2021), "Modeling of biofilm growth and the related changes in hydraulic properties of porous media", *Membr. Water Treat.*, **12**(5), 217–225. https://doi.org/10.12989/MWT.2021.12.5.217

Song, W., Lade, H., Yu, Y. and Kweon, J. (2018), "Effects of N-acetylcysteine on biofilm formation by MBR sludge",

*Membr. Water Treat.*, **9**(3), 195-203.
https://doi.org/10.12989/mwt.2018.9.3.195

Stewart, C.R., Muthye, V. and Cianciotto, N.P. (2012), "*Legionella pneumophila* persists within biofilms formed by *Klebsiella pneumoniae*, *Flavobacterium sp.*, and *Pseudomonas fluorescens* under dynamic flow conditions", *PloS one*, **7**(11), e50560. https://doi.org/10.1371/journal.pone.0050560

Tan, C.H., Koh, K.S., Xie, C., Tay, M., Zhou, Y., Williams, R., Ng, W.J., Rice, S.A. and Kjelleberg, S. (2014), "The role of quorum sensing signalling in EPS production and the assembly of a sludge community into aerobic granules", *The ISME J*, **8**(6), 1186-1197. https://doi.org/10.1038/ismej.2013.240

Wang, Y., Zhong, C., Huang, D., Wang, Y. and Zhu, J. (2013), "The membrane fouling characteristics of MBRs with different aerobic granular sludges at high flux", *Bioresour. Technol.*, **136**, 488-495. https://doi.org/10.1016/j.biortech.2013.03.066

Waters, C.M. and Bassler, B.L. (2005), "Quorum sensing: Cell-to-cell communication in bacteria", *Annual Rev. Cell Develop. Biol.*, **21**, 319-346.
https://doi.org/10.1146/annurev.cellbio.21.012704.131001

Wilen, B.M., Liebana, R., Persson, F., Modin, O. and Hermansson, M. (2018), "The mechanisms of granulation of activated sludge in wastewater treatment, its optimization, and impact on effluent quality", *Appl. Microbiol. Biotechnol.*, **102**(12), 5005-5020. https://doi.org/10.1007/s00253-018-8990-9

Yang, X., Beyenal, H., Harkin, G and Lewandowski, Z. (2000), "Quantifying biofilm structure using image analysis", *J. Microbiol. Method*, **39**(2), 109-119.
https://doi.org/10.1016/S0167-7012(99)00097-4

Yeon, K.M., Cheong, W.S., Oh, H.S., Lee, W.N., Hwang, B.K., Lee, C.H., Beyenal, H. and Lewandowski, Z. (2009), "Quorum sensing: A new biofouling control paradigm in a membrane bioreactor for advanced wastewater treatment", *Environ. Sci. Technol.*, **43**(2), 380-385. https://doi.org/10.1021/es8019275

Zhang, W., Liang, W., Zhang, Z. and Hao, T. (2021), "Aerobic granular sludge (AGS) scouring to mitigate membrane fouling: Performance, hydrodynamic mechanism and contribution quantification model", *Water Res.*, **188**, 116518. https://doi.org/10.1016/j.watres.2020.116518

Zhu, Y.L., Hou, H.M., Zhang, G.L., Wang, Y.F. and Hao, H.S. (2019), "AHLs regulate biofilm formation and swimming motility of Hafnia alvei H4", *Front. Microbiol.*, **10**, 1330. https://doi.org/10.3389/fmicb.2019.01330

*SP*